Kaposi's Sarcoma-associated Herpesvirus Viral Interleukin 6 Signaling Increases Integrin Beta 3 Levels and is Dependent on STAT3

Ricardo Rivera-Soto,[a,b] Nathan J. Dissinger,[a] and Blossom Damania[a,b,c,#]

a. Lineberger Comprehensive Cancer Center, University of North Carolina at Chapel Hill, Chapel Hill, North Carolina, USA
b. Curriculum in Genetics and Molecular Biology, University of North Carolina at Chapel Hill, Chapel Hill, North Carolina, USA
c. Department of Microbiology and Immunology, University of North Carolina at Chapel Hill, Chapel Hill, North Carolina, USA

Running title: The KSHV protein vIL-6 induces integrin β3

[#]Address correspondence to Blossom Damania, blossom_damania@med.unc.edu (BD)

N.J.D. and R.R. contributed equally to this work

Abstract Word Count: 239/250 Importance Word count: 113/150 Text Word Count: 4214/5000

ABSTRACT

Kaposi's sarcoma-associated herpesvirus (KSHV) is the causative agent of two B-cell lymphoproliferative diseases and Kaposi's sarcoma, an endothelial-cell driven cancer. KSHV viral interleukin-6 (vIL-6) is a viral homolog of human IL-6 that is expressed in KSHV-associated malignancies. Previous studies have shown that the expression of the integrin β3 (ITGB3) subunit is induced upon KSHV infection and that this integrin is involved in KSHV entry into adherent cells. Here, we report that KSHV vIL-6 is able to induce the expression of ITGB3 and increase surface expression of the $\alpha V\beta 3$ integrin heterodimer. We demonstrate using siRNA depletion and inhibitor studies that KSHV vIL-6 can increase ITGB3 by inducing STAT3 signaling. Furthermore, we found that secreted vIL-6 is capable of inducing ITGB3 in endothelial cells in an intercellular manner. Importantly, the ability to induce ITGB3 in endothelial cells seems to be specific to vIL-6 as over-expression of hIL-6 alone did not affect levels of the integrin. Our lab and others have previously shown that vIL-6 can induce angiogenesis, and we investigated whether ITGB3 was involved in this process. We found that siRNA depletion of ITGB3 in vIL-6-expressing endothelial cells resulted in a decrease in adhesion to extracellular matrix proteins. Moreover, depletion of ITGB3 hindered the ability of vIL-6 to promote angiogenesis as measured by a tubule formation assay. In conclusion, we found that vIL-6 can singularly induce ITGB3 and that this induction is dependent on vIL-6 activation of the STAT3 signaling pathway.

IMPORTANCE

Kaposi's sarcoma-associated herpesvirus (KSHV) is the etiologic agent of three human malignancies: multicentric Castleman's disease, primary effusion lymphoma, and Kaposi's sarcoma. Kaposi's sarcoma is a highly angiogenic tumor that arises from endothelial cells. It has been previously reported that KSHV infection of endothelial cells leads to an increase of integrin $\alpha V\beta 3$, a molecule observed to be involved in the angiogenic process of several malignancies. Our data demonstrate that the KSHV protein, viral interleukin-6 (vIL-6) can induce integrin $\beta 3$ in an intracellular and intercellular manner. Furthermore, we showed that this induction is necessary for vIL-6-mediated cell adhesion and angiogenesis, suggesting a potential role of integrin $\beta 3$ in KSHV pathogenesis and development of Kaposi's sarcoma.

INTRODUCTION

Integrins are heterodimeric membrane glycoproteins that consist of an alpha and a beta subunit. These cell surface proteins are receptors for extracellular matrix proteins, growth factors, cytokines, immunoglobulins and matrix-degrading proteases (1). One of the beta subunits, β3, can dimerize with αIIb in platelets and αV in other cell types, including endothelial cells. Integrin αVβ3 binds to adhesive proteins such as von Willebrand factor, fibrinogen, and fibronectin. The binding of these ligands can induce the "outside-inside" signaling through the integrin, resulting in endothelial cell migration (2), angiogenesis (2, 3), and TGF-β1 signaling (4, 5). Integrin αVβ3 expression and function are of significant interest as expression is upregulated in several forms of cancer and correlates with progression of malignancies (1, 6).

A receptor for cellular proteins, integrin αVβ3 has also been reported to be a receptor for viruses, including Kaposi's sarcoma-associated herpesvirus (KSHV), also known as human herpesvirus-8 (HHV-8) (7-9). KSHV is a double-stranded DNA virus and member of the gammaherpesvirus family (10) that was first isolated from a Kaposi's sarcoma (KS) patient and found to be the causative agent of this cancer (11). Subsequently, it was demonstrated that KSHV also causes the B-cell malignancy primary effusion lymphoma (PEL) (12), and it is associated with the proliferative disorder multicentric Castleman's disease (MCD) (13). DiMaio and colleagues reported that latent infection of KSHV increases integrin β3 (ITGB3) expression in endothelial cells (14). This increase causes the infected cells to bind more strongly to select extracellular matrix (ECM) components. Additionally, knockdown of *ITGB3* results in a

decreased ability of infected cells to form tubules in an *in vitro* model of angiogenesis. These data suggest that KSHV upregulates *ITGB3*, which can play a role in the angiogenic processes of KSHV-infected endothelial cells (14). However, the mechanism by which the virus mediates the induction of ITGB3 has not been characterized.

KSHV encodes over 80 open reading frames (ORFs), which consist of latent and lytic genes. Most infected cells contain a latent virus, expressing only a small subset of genes that encode proteins and microRNAs. Upon reactivation, the virus starts expressing lytic genes in an ordered fashion and produces new viral progeny (15). ORF K2 encodes for viral interleukin-6 (vIL-6), a homolog of human IL-6 (hIL-6) (16-18). During latency, vIL-6 expression is detected at low levels, but it significantly increases during lytic replication. Similar to hIL-6, secreted vIL-6 binds to the IL-6 receptor (IL-6R, composed of gp80 and gp130 subunits) and induces the JAK/STAT signaling cascade (18, 19). However, while the cell readily secretes hIL-6, vIL-6 is mainly localized to the endoplasmic reticulum (ER). Here, vIL-6 interacts with gp130, a component of the IL-6R, and induces JAK/STAT signaling in an intracellular manner (20). Through activation of transcription factor STAT3, vIL-6 induces cell proliferation (18, 21, 22) as well as migration (22-24). vIL-6 also induces angiogenesis and hematopoiesis, aiding in the growth of tumors (25).

Herein, we report that vIL-6 is capable of inducing ITGB3 at the mRNA and protein levels. Phosphorylation of STAT3 is required for this induction, as indicated by assays using drug inhibitors and siRNA knockdowns. Interestingly, vIL-6 is a stronger inducer of

ITGB3 when compared to the human homolog, even though both are capable of inducing STAT3 signaling. Finally, we show how this phenotype may promote KSHV pathogenesis by contributing to angiogenesis. These studies highlight vIL-6 as a player in KSHV-induced ITGB3.

RESULTS

Viral IL-6-expressing cells have increased levels of ITGB3. Our lab has previously reported microarray data that indicated human umbilical vein endothelial cells (HUVECs) stably expressing vIL-6 had increased levels of *ITGB3* mRNA compared to cells expressing the empty vector (EV) (24). High levels of *ITGB3* expression in vIL-6-expressing HUVECs were confirmed with RT-qPCR (Fig. 1A). We next performed immunoblots probing for ITGB3 and found that the protein level was also increased in the vIL-6-HUVECs (Fig. 1B). Additionally, we wanted to know whether the higher levels of *ITGB3* mRNA and protein were due to an increased ITGB3 transcription. To test this, we attempted to transfect the stable EV- and vIL-6-HUVECs with an ITGB3-luciferase reporter plasmid. However, the transfection efficiency in HUVECs was low, and thus we opted to use HEK293T cells. HEK293T cells were co-transfected with a vIL-6-expressing plasmid or the corresponding EV control and the luciferase reporter plasmid. Expression of vIL-6, as detected by immunoblotting, led to an increase in the expression of luciferase (Fig. 1C). The results suggest that vIL-6 promotes the activation of the ITGB3 promoter and consequently increasing the mRNA and protein levels.

The previous observation, however, only examined the total amount of ITGB3 protein within the cell. To determine if this increase in total ITGB3 resulted in increased surface expression, we performed flow cytometry analysis using an $\alpha V\beta 3$ antibody. Histograms comparing the geometric means of fluorescence intensity indicate that vIL-6-HUVECs have a two-fold increase in levels of surface $\alpha V\beta 3$ integrin (Fig. 1D). Altogether, these results are reminiscent of those reported by DiMaio et al., where KSHV infection of endothelial cells led to a significant increase in total ITGB3 expression, but only a modest increase of surface expression (14).

Viral IL-6-expressing cells can induce ITGB3 expression in an intercellular manner. We next wanted to determine whether vIL-6-expressing endothelial cells induce ITGB3 through intercellular signaling. To explore this possibility, we collected conditioned medium (CM) from both the EV- and vIL-6-HUVECs and added them to naïve hTERT-HUVECs at a 1:1 ratio with fully supplemented medium. After 24 hours, we were able to detect an increase in *ITGB3* mRNA (Fig. 2A) and protein (Fig. 2B) from the hTERT-HUVECs that were treated with the vIL-6-containing conditioned medium.

KSHV-infected endothelial cells have been reported not to express high levels of vIL-6. In addition to endothelial cells, B-cells are another cell type that is readily infected *in vivo* (26-28). Importantly, KSHV-infected cells involved in MCD or PEL, two KSHV-etiological malignancies that are made primarily of B-cells, express higher amounts of vIL-6 than do KS tumor cells (29). Furthermore, in KS lesions, the cells that express the highest quantities of vIL-6 are from invading lymphocytes (30). For these reasons, we

created BJABs, a B-cell line that constitutively expresses EV or vIL-6. Conditioned medium from these vIL-6-expressing BJAB cells induced *ITGB3* mRNA and protein expression in hTERT-HUVECs similarly to what we observed from the HUVEC-conditioned medium (Fig. 2C and 2D).

To determine whether secreted vIL-6 was needed for the induction of ITGB3 or if it was another secreted factor from stable vIL-6 cells, we performed a neutralization assay (Fig. 2E). Conditioned media were created that contained no antibody supplement, mouse non-specific IgG, or mouse α-vIL-6 IgG. These conditioned media were then placed on naïve hTERT-HUVECs, further supplemented with antibody, and incubated for 24 hours. As expected, cells treated with the EV-conditioned media, regardless of the antibody supplement, did not induce ITGB3. On the other hand, cells that were treated with the mock or non-specific antibody containing vIL-6-HUVEC-conditioned media had increased levels of ITGB3. However, cells that were treated with the vIL-6-HUVEC-conditioned medium that contained the vIL-6 specific antibody had ITGB3 levels similar to the EV-conditioned-medium-treated cells. These results demonstrate that secreted vIL-6 is involved in the induction of ITGB3.

STAT3 signaling is necessary for vIL-6-mediated ITGB3 induction. A previous report examining the effect of high $\alpha V\beta 3$ integrin levels in breast cancer cells found that STAT3 contributes to the invasiveness of the cells (31). This finding indicated to us a possible link between STAT3 and $\alpha V\beta 3$ activity. Since it is well established that vIL-6 induces STAT3 signaling (19, 32), we wanted to examine the relationship between

STAT3 and ITGB3 in vIL-6-expressing cells. We first treated EV- and vIL-6-HUVECs with the STAT3 inhibitor cryptotanshinone. After 48 hours, we observed the expected decrease in STAT3 phosphorylation as well as a decrease in total ITGB3 expression (Fig. 3A). This result indicates that vIL-6-induced STAT3 signaling is essential for ITGB3 induction. To confirm this data, we transfected cells with a STAT3-specific siRNA and observed the same loss of ITGB3 levels in the vIL-6-HUVECs (Fig. 3B). We then performed a similar experiment in which naïve hTERT-HUVECs were first transfected with the STAT3 siRNA, followed by treatment with EV- or vIL-6- conditioned medium. We observed an increase in ITGB3 protein levels only in cells that were treated with vIL-6-containing conditioned medium, and that expressed STAT3 (Fig. 3C). These results suggest that activation of STAT3 is necessary for the ability of vIL-6 to induce ITGB3.

Human IL-6 is not a strong inducer of ITGB3 as is vIL-6. Since vIL-6 and hIL-6 can both activate STAT3, we hypothesized that hIL-6 would induce ITGB3, as well. To test this hypothesis, we collected lysates from HUVECs expressing EV, vIL-6, or hIL-6 and performed immunoblots (Fig. 4A). Surprisingly, although the expression of hIL-6 in HUVECs slightly increased the levels of phosphorylated STAT3, it did not affect levels of ITGB3. To confirm these results, the stable HUVECs were supplemented for 48 hours with recombinant (r) hIL-6. The results indicated that, even in the presence of rhIL-6, levels of ITGB3 are increased only in the vIL-6-expressing cells. We next made conditioned medium from HUVECs and BJABs that contained EV, vIL-6 or hIL-6. These conditioned media were then used to treat hTERT-HUVECs for 24 hours, after which the lysates were collected (Fig. 4B). Again, we observed a substantial increase in

ITGB3 protein levels induced by the vIL-6-conditioned medium. Cells that were treated with the EV- or hIL-6-conditioned medium ranged from no increase to a very modest increase in ITGB3 protein.

The induction of signaling pathways by hIL-6 can occur through two different but similar mechanisms known as *classical*- and *trans*-signaling *(33, 34)*. In classical-signaling, hIL-6 binds to membrane-bound IL-6Rα (gp80), which interacts with gp130, leading to the intracellular activation of the JAK/STAT signaling pathway. This process is restricted to cells that express the membrane-bound receptor. In contrast, the trans-signaling pathway occurs when secreted hIL-6 binds to the soluble form of the IL-6Rα. This hIL-6/sIL-6R complex binds gp130 and induces activation of the JAK/STAT signaling pathway. Importantly, since gp130 is ubiquitously expressed, this process can take place even in cells that lack expression of the membrane-bound IL-6R.

Recently, it was shown that HUVECs could support both mechanisms, but activation of the trans-signaling pathway by treating cells with both recombinant hIL-6 and sIL-6R led to higher and longer activation of STAT3 (35). For this reason, we hypothesized that supplementing cells for 24 hours with both hIL-6 and sIL-6Rα will result in high levels of activated STAT3 and thus ITGB3. Immunoblots show that EV-HUVECs treated with both recombinant proteins resulted in an increase in phosphorylated STAT3, confirming activation of the pathway (Fig. 4C). Importantly, this activation also increased ITGB3 levels similar to those in the vIL-6-expressing cells (Fig. 4C). However, addition of the recombinant proteins did not enhance vIL-6-mediated induction of ITGB3. Altogether,

the data suggest that in endothelial cells, activation of IL-6R plays a crucial role in induction of ITGB3, and in comparison to its cellular homolog, vIL-6 can accomplish this even in the absence of soluble IL-6Rα.

Integrin β3 expression increases vIL-6-HUVEC adhesion. DiMaio et al. demonstrated that KSHV-infected endothelial cells adhere more readily to the ECM proteins fibronectin and vitronectin (14). This increase in adhesion could be inhibited by the addition of RGD peptides, which interfere with several integrin-ECM interactions. We wanted to examine if the increased amount of ITGB3 in vIL-6-HUVECs resulted in increased adherence to fibronectin and vitronectin. EV- and vIL-6-HUVECs were transfected with non-targeting control (NTC) or an *ITGB3*-targeting pool of siRNAs (Fig. 5A). Cells were stained with a fluorescent dye and then allowed to adhere to wells coated with fibronectin or vitronectin (Fig. 5B and 5C, respectively). We found that vIL-6-HUVECs transfected with NTC siRNAs had an increase in adherence to fibronectin-coated wells, but relatively the same adherence to vitronectin as compared to EV-HUVECs. However, when *ITGB3* was knocked down in vIL-6-HUVECs the fluorescent signal indicating the number of attached cells decreased by statistically significant levels for both ECM components, whereas the signal for EV-HUVECs did not show a significant decrease. These results indicate that vIL-6 expression makes cell attachment to the ECM components fibronectin and vitronectin more heavily dependent on ITGB3.

Viral IL-6-induced tubule formation is mediated through ITGB3. vIL-6 has been previously reported to aid in angiogenesis (25, 36, 37). Since KS is highly vascularized,

and DiMaio et al. demonstrated that *ITGB3* knockdown decreased tubule formation of latently KSHV-infected endothelial cells, we sought to see if this was the case for vIL-6-expressing cells, as well. EV- and vIL-6-HUVECs were treated with NTC or ITGB3 siRNAs for 48 hours. Cells were then placed on top of Matrigel and incubated for up to four hours. The number of branching points was manually calculated from at least thirty-two images. The results showed that vIL-6-HUVECs transfected with NTC siRNA had significantly more branch points than EV-HUVECs (Fig. 6A and 6B). The number of branching points, however, significantly decreased when *ITGB3* was knocked down in vIL-6-HUVECs; this decrease was not observed in *ITGB3*-knockdown EV-HUVECs. These results indicate that ITGB3 is involved in vIL-6-mediated endothelial tubule formation, suggesting a possible role for ITGB3 in KSHV-induced angiogenesis.

DISCUSSION

The heterodimer $\alpha V\beta 3$ integrin is hypothesized to be important in several cancers and viral infections. A role for $\alpha V\beta 3$ integrin has been suggested in KSHV pathogenesis, specifically viral infection (7-9) and angiogenesis (14). Though KSHV infection has been demonstrated to induce ITGB3 (14), and the viral protein gB shown to interact with integrin $\alpha V\beta 3$ (8), no specific KSHV protein has been identified as responsible for ITGB3 induction. In this report, we confirm our previous microarray data that identified *ITGB3* as highly upregulated in vIL-6-expressing HUVECs (24) and demonstrate that stable expression of this viral protein in endothelial cells results in an increase of total and cellular-surface-targeted ITGB3 protein (Fig. 7). We have also demonstrated that vIL-6 can be secreted from endothelial or B-cells and induce *ITGB3* at the mRNA and

protein levels in naïve endothelial cells. These results are relevant because vIL-6 can be found circulating in the blood of KSHV and HIV co-infected individuals (38, 39), and its paracrine signaling is believed to play a significant role in viral pathogenesis (40).

Since vIL-6 is known to induce the activation of the JAK/STAT signaling pathway (19, 32), we sought to determine if this pathway is involved in ITGB3 induction. We found that phosphorylated STAT3 is required for vIL-6 specific induction of ITGB3. To our knowledge, this is the first report to demonstrate a mechanism of ITGB3 expression that requires STAT3 signaling. Interestingly, neither overexpression of the cellular homolog nor treatment with recombinant hIL-6 in endothelial cells induced ITGB3 expression. A possible explanation for this result is that HUVECs are more responsive to hIL-6 trans-signaling activation that relies on the binding of the cytokine to soluble, rather than to membrane-bound, IL-6R (34, 35). Despite the slight activation of STAT3, levels of ITGB3 were not increased in the presence of hIL-6. Importantly, this was circumvented when cells were supplemented with a recombinant, soluble IL-6Rα that increased the levels of ITGB3 to levels seen in vIL-6-expressing cells, confirming that induction of the pathway plays a significant role in modulating expression of ITGB3.

Activation of STAT3 signaling by hIL-6 alone in endothelial cells is not sufficient for ITGB3 induction, suggesting that vIL-6 overcomes the need for IL-6Rα (gp80) by consistently activating the pathway through gp130. Our results demonstrate that in endothelial cells this is a unique function of vIL-6 that has not been previously reported. Since KSHV can activate STAT3 in the absence of vIL-6 (41), and since two different

KSHV miRNAs that are latently expressed, have been shown to modulate STAT3 (42, 43), it would be interesting to determine whether vIL-6 is necessary for the KSHV-mediated induction of ITGB3 in infected endothelial cells.

After demonstrating induction of ITGB3 by vIL-6, we wanted to determine if this increase resulted in a functional phenotype. We have shown that vIL-6-expressing HUVECs treated with a non-targeting siRNA pool have a statistically significant higher binding affinity to the ECM proteins fibronectin and vitronectin than do vIL-6-HUVECs that have *ITGB3* knocked down. This significant decrease in binding with *ITGB3* knockdown was unique to the vIL-6 HUVECs compared to EV HUVECs. Furthermore, utilizing these siRNAs, we performed a tubule formation assay, an *in vitro* approach to measure angiogenic phenotype. The vIL-6-HUVECs that still expressed ITGB3 had more branching points than either EV-HUVEC or vIL-6-HUVECs treated with the ITGB3 siRNA. The ability of vIL-6-expressing HUVECs to have increased binding to fibronectin, which aids in the stability and growth of microvessels (44, 45), and increased endothelial cell branching only when ITGB3 is expressed, hints at the importance of this induction for angiogenesis.

Altogether, our data identify the KSHV protein vIL-6 as a bona fide inducer of ITGB3. The oncovirus KSHV's arsenal of proteins and non-coding RNAs exploits cellular pathways that facilitate pathogenesis, which can result in the development of tumors. We hypothesize that ITGB3 plays an important role in the capacity of the virus to induce angiogenesis and endothelial cell migration. The ability of vIL-6 to be secreted and

affect cells in a paracrine manner further confirms the essential role that infiltrating cells might play in KS lesions by enhancing cellular processes such as angiogenesis. In conclusion, this report further characterizes the role of vIL-6 in endothelial cells and its contribution to viral pathogenesis.

MATERIALS AND METHODS

Cell culture. Human telomerase reverse transcriptase-immortalized human umbilical vein endothelial cells (hTERT-HUVEC) were cultured in EBM-2 (Lonza) or ECGM2 (PromoCell) and their respective supplement kits as described previously (46). BJAB cells were maintained in RPMI 1640 medium (Corning). All media were supplemented with 10% heat-inactivated FBS, 1% penicillin/streptomycin, and 1% L-glutamine.

Production of lentivirus vectors and stable cell lines. Production of the empty vector (EV) and vIL-6 lentivirus and the construction of stable cell lines were described previously (23). The hIL-6 lentiviral vector was cloned similarly. Briefly, *hIL-6* was inserted into a lentivirus vector with puromycin resistance. Lentivirus was produced using ViraPower lentiviral expression system (Invitrogen), and cells were transduced by spin inoculation in the presence of polybrene (8 μg/mL). BJABs expressing EV, vIL-6 or hIL-6 were made using the same lentivirus and spin inoculation procedure.

RNA isolation and real-time qPCR. RNA was isolated from cells using the RNeasy Plus Mini Kit (Qiagen). cDNA was obtained from 1 μg total RNA using the iScript cDNA Synthesis kit (Bio-Rad). At least three biological replicates were performed for each

condition used in experiments, with three technical replicates for each sample. Real-time qPCR was performed on a Quantstudio 6 Flex Real-Time PCR machine (ThermoFisher) using SensiFAST SYBR Lo-Rox real-time PCR master mix (Bioline). PCR primer sequences used for ITGB3 were obtained from (47). To amplify actin cDNA, the forward primer 5'-TCATGAAGTGTGACGTGGACATC-3' and reverse primer 5'-CAGGAGGAGCAATGATCTTGATCT-3' were used.

Immunoblotting. Cells were collected, and lysates were prepared from washed pellets using NP-40 lysis buffer (0.1% NP-40, 150 mM NaCl, 50 mM Tris HCl pH 8.0, 30 mM β-glycerophosphate, 50 mM NaF, 1 mM Na_3VO_4, 1 Roche protease inhibitor tablet per 50 mL). Samples were clarified by centrifugation at 16,000 x g for 10-15 minutes, and protein concentration was determined by Bradford assay (Bio-Rad). Lysates were resolved on acrylamide SDS-PAGE gels. ITGB3 (4702S), pSTAT3 Y705 (9131S), total STAT3 (4904S), and secondary HRP-conjugated antibodies (anti-rabbit (7074) and anti-mouse (7076)) were purchased from Cell Signaling Technology (CST). Human IL-6 antibodies were obtained from Origene (TA300413) and CST (12153S). The vIL-6 antibody was purified from the supernatant of v6m 12.1.1 hybridomas (ATCC) (48) using magnetic Protein A/G beads (Thermo Fisher). Actin (SC-1615) antibody conjugated with HRP was purchased from Santa Cruz Biotechnology.

Luciferase reporter assay. Two hundred thousand HEK293T cells were plated per well into a 24-well plate. Twenty-four hours post-seeding, cells were co-transfected with 500 ng/well of a vIL-6-expressing plasmid or the corresponding empty vector (EV)

backbone (a gift from Britt Glausinger) (49), and 150 ng/well of the ITGB3-luciferase reporter plasmid (HPRM23183-PG04) purchased from GeneCopoeia. Transfection was performed with Lipofectamine 3000 according to the manufacturers' protocol. Supernatants were collected 48 hours post-transfection. The *Gaussia* luciferase and the internal control, secreted embryonic alkaline phosphatase (SEAP), were measured using the Secrete-Pair™ Dual Luminescence Assay Kit (GeneCopoeia) according to the manufacturers' protocol. To confirm vIL-6 expression, protein lysates were prepared and immunoblots performed as described.

Flow cytometry. Endothelial cells were plated after trypsinization and incubated for 48 hours. Cells were then collected using Versene and counted. Five hundred thousand cells per sample were washed and resuspended in 80 μL of FACS buffer (PBS + 2% FBS + 2 mM EDTA) along with 20 μL human FcR Blocking Reagent (MACS Miltenyi Biotec), then allowed to incubate for 10 minutes at 4°C. Cells were then spun down and stained with 2 μg αVβ3 antibodies (MAB1976, MilliporeSigma) in 100 μL FACS buffer and incubated on ice in the dark for 30 minutes. After primary staining, cells were washed three times, then stained for 30 minutes on ice in the dark with 300 ng goat α-mouse antibody conjugated with AF488 fluorophore (Thermo Fisher). After washing off the excess secondary stain, cells were fixed in FACS buffer containing 1% formaldehyde. Samples were run on a MACSQuant VYB flow cytometer (Miltenyi Biotec). The analysis was conducted using FlowJo software.

Conditioned medium preparation and treatment. HUVEC and BJAB stable cell lines were incubated for 24 hours in serum- or supplement-free medium. The medium was then collected, centrifuged and then added to naïve HUVEC cells at a 1:1 ratio with completed medium. Lysates were harvested 24 hours post-treatment.

Neutralization antibody assay. Conditioned media from stable HUVECs were created as stated above with the exception of certain wells that received 10 μg mouse non-specific IgG (Santa Cruz Biotechnology) or 10 μg purified vIL-6 antibody. Conditioned medium was then added to hTERT-HUVECs and re-supplemented with the antibody. After a 24-hour incubation, lysates were collected and immunoblots performed.

siRNA transfections and drug inhibitor treatment. siRNAs were transfected into cells using Lipofectamine RNAiMax reagent (Thermo Fisher) and allowed to incubate for 48 hours before lysate collection or cell use in other assays. ON-TARGETplus SMARTpool siRNAs for human ITGB3 (L004124), as well as the non-targeting control (D001810) siRNAs, were purchased from Dharmacon. Silencer Select siRNA targeting STAT3 (4390824), as well as the respective negative control, were obtained from ThermoFisher. For STAT3 drug inhibition, cells were treated with 20 μM of cryptotanshinone (MedChemExpress) or vehicle (DMSO). Cells were incubated for 48 hours post-treatment before lysates were collected.

Recombinant human IL-6 and sIL-6Rα treatment. For hIL-6 treatment, HUVECs were plated on six-well plates with complete medium. Twenty-four hours after plating, the

398 medium was replaced with fresh medium containing rhIL-6 (Peprotech) at the indicated
399 concentrations. After incubating cells for 48 hours with rhIL-6, lysates were prepared
400 and immunoblots performed as described above. For the experiment with sIL-6Rα, cells
401 were treated for 24 hours similarly to above, but in the presence or absence of sIL-6Rα
402 (GenScript).
403
404 **Adhesion assay.** Cells were plated in 100 mm dishes and transfected the next day with
405 siRNAs as stated above. Cells were removed from the plate using Versene and washed
406 in PBS twice. Cells were resuspended in 500 μL serum-free medium at a concentration
407 of 10^6 cells/mL. Two and a half microliters of the fluorescent dye calcein AM, obtained
408 from Invitrogen Vybrant Cell Adhesion Kit (Thermo Fisher), was added to the cell
409 suspension and incubated for 30 minutes at 37°C. During the incubation, 8-well strips
410 that contained either fibronectin or vitronectin (Millicoat Cell Adhesion strips, Millipore)
411 were allowed to warm up to room temperature and washed in PBS. After the 30-minute
412 incubation, cells were washed in prewarmed medium three times, then diluted to 10^5
413 cells/mL and 100 μL added to each well. The cells were allowed to adhere to the ECM
414 components for 30 minutes at 37°C. Nonadherent cells were removed by gentle
415 washing (repeated five times) in a warmed medium. After the final wash, 200 μL PBS
416 was added to each well, and the fluorescence was measured on a CLARIOstar plate
417 reader (BMG Labtech).
418
419 **Tubule formation assay.** Empty vector- or vIL-6-HUVECs were plated and transfected
420 with siRNAs as indicated above. Forty-eight hours post-transfection, cells were

detached from the plates, counted, and 1.25 x 10^5 cells in a total of 1 ml complete medium were seeded on top of 300 µl Matrigel (Corning) in the wells of a 24-well plate. At least four images were taken per each well between 3- and 4-hours post-seeding, and the number of branching points was manually calculated using ImageJ.

Statistics. Statistics were calculated using the Kruskal-Wallis function in GraphPad.

ACKNOWLEDGMENTS:

We are thankful to the Damania Lab member Whitney Tevebaugh for revising and editing the manuscript. This work was supported by public health service grants CA096500, CA019014, DE028211, and CA163217. BD is a Leukemia and Lymphoma Society Scholar, and a Burroughs Wellcome Fund Investigator in Infectious Disease. RR was supported by NIH grant GM007092. The funders had no role in the design, collection, or interpretation of the study.

REFERENCES:

1. **Danhier F, Le Breton A, Preat V.** 2012. RGD-based strategies to target alpha(v) beta(3) integrin in cancer therapy and diagnosis. Mol Pharm **9:**2961-2973.
2. **Brooks PC, Clark RA, Cheresh DA.** 1994. Requirement of vascular integrin alpha v beta 3 for angiogenesis. Science **264:**569-571.
3. **Brooks PC, Montgomery AM, Rosenfeld M, Reisfeld RA, Hu T, Klier G, Cheresh DA.** 1994. Integrin alpha v beta 3 antagonists promote tumor regression by inducing apoptosis of angiogenic blood vessels. Cell **79:**1157-1164.
4. **Feng XX, Liu M, Yan W, Zhou ZZ, Xia YJ, Tu W, Li PY, Tian DA.** 2013. beta3 integrin promotes TGF-beta1/H2O2/HOCl-mediated induction of metastatic phenotype of hepatocellular carcinoma cells by enhancing TGF-beta1 signaling. PLoS One **8:**e79857.

5. **Rapisarda V, Borghesan M, Miguela V, Encheva V, Snijders AP, Lujambio A, O'Loghlen A.** 2017. Integrin Beta 3 Regulates Cellular Senescence by Activating the TGF-beta Pathway. Cell Rep **18:**2480-2493.
6. **Nieberler M, Reuning U, Reichart F, Notni J, Wester HJ, Schwaiger M, Weinmuller M, Rader A, Steiger K, Kessler H.** 2017. Exploring the Role of RGD-Recognizing Integrins in Cancer. Cancers (Basel) **9**.
7. **Veettil MV, Sadagopan S, Sharma-Walia N, Wang FZ, Raghu H, Varga L, Chandran B.** 2008. Kaposi's sarcoma-associated herpesvirus forms a multimolecular complex of integrins (alphaVbeta5, alphaVbeta3, and alpha3beta1) and CD98-xCT during infection of human dermal microvascular endothelial cells, and CD98-xCT is essential for the postentry stage of infection. J Virol **82:**12126-12144.
8. **Garrigues HJ, Rubinchikova YE, Dipersio CM, Rose TM.** 2008. Integrin alphaVbeta3 Binds to the RGD motif of glycoprotein B of Kaposi's sarcoma-associated herpesvirus and functions as an RGD-dependent entry receptor. J Virol **82:**1570-1580.
9. **Garrigues HJ, DeMaster LK, Rubinchikova YE, Rose TM.** 2014. KSHV attachment and entry are dependent on alphaVbeta3 integrin localized to specific cell surface microdomains and do not correlate with the presence of heparan sulfate. Virology **464-465:**118-133.
10. **Renne R, Lagunoff M, Zhong W, Ganem D.** 1996. The size and conformation of Kaposi's sarcoma-associated herpesvirus (human herpesvirus 8) DNA in infected cells and virions. J Virol **70:**8151-8154.
11. **Chang Y, Cesarman E, Pessin MS, Lee F, Culpepper J, Knowles DM, Moore PS.** 1994. Identification of herpesvirus-like DNA sequences in AIDS-associated Kaposi's sarcoma. Science **266:**1865-1869.
12. **Cesarman E, Chang Y, Moore PS, Said JW, Knowles DM.** 1995. Kaposi's sarcoma-associated herpesvirus-like DNA sequences in AIDS-related body-cavity-based lymphomas. N Engl J Med **332:**1186-1191.
13. **Soulier J, Grollet L, Oksenhendler E, Cacoub P, Cazals-Hatem D, Babinet P, d'Agay MF, Clauvel JP, Raphael M, Degos L, et al.** 1995. Kaposi's sarcoma-associated herpesvirus-like DNA sequences in multicentric Castleman's disease. Blood **86:**1276-1280.
14. **DiMaio TA, Gutierrez KD, Lagunoff M.** 2011. Latent KSHV infection of endothelial cells induces integrin beta3 to activate angiogenic phenotypes. PLoS Pathog **7:**e1002424.
15. **Damania B, Cesarman E.** 2013. Kaposi's Sarcoma-Associated Herpesvirus, p 2080-2128, Fields Virology. Lippincott Willams & Wilkins.
16. **Moore PS, Boshoff C, Weiss RA, Chang Y.** 1996. Molecular mimicry of human cytokine and cytokine response pathway genes by KSHV. Science **274:**1739-1744.
17. **Neipel F, Albrecht JC, Ensser A, Huang YQ, Li JJ, Friedman-Kien AE, Fleckenstein B.** 1997. Human herpesvirus 8 encodes a homolog of interleukin-6. J Virol **71:**839-842.
18. **Nicholas J, Ruvolo VR, Burns WH, Sandford G, Wan X, Ciufo D, Hendrickson SB, Guo HG, Hayward GS, Reitz MS.** 1997. Kaposi's sarcoma-associated human herpesvirus-8 encodes homologues of macrophage inflammatory protein-1 and interleukin-6. Nat Med **3:**287-292.

19. **Molden J, Chang Y, You Y, Moore PS, Goldsmith MA.** 1997. A Kaposi's sarcoma-associated herpesvirus-encoded cytokine homolog (vIL-6) activates signaling through the shared gp130 receptor subunit. J Biol Chem **272:**19625-19631.
20. **Chen D, Sandford G, Nicholas J.** 2009. Intracellular signaling mechanisms and activities of human herpesvirus 8 interleukin-6. J Virol **83:**722-733.
21. **Burger R, Neipel F, Fleckenstein B, Savino R, Ciliberto G, Kalden JR, Gramatzki M.** 1998. Human herpesvirus type 8 interleukin-6 homologue is functionally active on human myeloma cells. Blood **91:**1858-1863.
22. **Wu J, Xu Y, Mo D, Huang P, Sun R, Huang L, Pan S, Xu J.** 2014. Kaposi's sarcoma-associated herpesvirus (KSHV) vIL-6 promotes cell proliferation and migration by upregulating DNMT1 via STAT3 activation. PLoS One **9:**e93478.
23. **Giffin L, Yan F, Ben Major M, Damania B.** 2014. Modulation of Kaposi's sarcoma-associated herpesvirus interleukin-6 function by hypoxia-upregulated protein 1. J Virol **88:**9429-9441.
24. **Giffin L, West JA, Damania B.** 2015. Kaposi's Sarcoma-Associated Herpesvirus Interleukin-6 Modulates Endothelial Cell Movement by Upregulating Cellular Genes Involved in Migration. MBio **6:**e01499-01415.
25. **Aoki Y, Jaffe ES, Chang Y, Jones K, Teruya-Feldstein J, Moore PS, Tosato G.** 1999. Angiogenesis and hematopoiesis induced by Kaposi's sarcoma-associated herpesvirus-encoded interleukin-6. Blood **93:**4034-4043.
26. **Whitby D, Howard MR, Tenant-Flowers M, Brink NS, Copas A, Boshoff C, Hatzioannou T, Suggett FE, Aldam DM, Denton AS, et al.** 1995. Detection of Kaposi sarcoma associated herpesvirus in peripheral blood of HIV-infected individuals and progression to Kaposi's sarcoma. Lancet **346:**799-802.
27. **Huang YQ, Li JJ, Poiesz BJ, Kaplan MH, Friedman-Kien AE.** 1997. Detection of the herpesvirus-like DNA sequences in matched specimens of semen and blood from patients with AIDS-related Kaposi's sarcoma by polymerase chain reaction in situ hybridization. Am J Pathol **150:**147-153.
28. **Ambroziak JA, Blackbourn DJ, Herndier BG, Glogau RG, Gullett JH, McDonald AR, Lennette ET, Levy JA.** 1995. Herpes-like sequences in HIV-infected and uninfected Kaposi's sarcoma patients. Science **268:**582-583.
29. **Staskus KA, Sun R, Miller G, Racz P, Jaslowski A, Metroka C, Brett-Smith H, Haase AT.** 1999. Cellular tropism and viral interleukin-6 expression distinguish human herpesvirus 8 involvement in Kaposi's sarcoma, primary effusion lymphoma, and multicentric Castleman's disease. J Virol **73:**4181-4187.
30. **Cannon JS, Nicholas J, Orenstein JM, Mann RB, Murray PG, Browning PJ, DiGiuseppe JA, Cesarman E, Hayward GS, Ambinder RF.** 1999. Heterogeneity of viral IL-6 expression in HHV-8-associated diseases. J Infect Dis **180:**824-828.
31. **Mierke CT.** 2013. The integrin alphav beta3 increases cellular stiffness and cytoskeletal remodeling dynamics to facilitate cancer cell invasion. New Journal of Physics **15:**015003-015024.
32. **Wan X, Wang H, Nicholas J.** 1999. Human herpesvirus 8 interleukin-6 (vIL-6) signals through gp130 but has structural and receptor-binding properties distinct from those of human IL-6. J Virol **73:**8268-8278.

33. **Scheller J, Chalaris A, Schmidt-Arras D, Rose-John S.** 2011. The pro- and anti-inflammatory properties of the cytokine interleukin-6. Biochim Biophys Acta **1813:**878-888.
34. **Scheller J, Garbers C, Rose-John S.** 2014. Interleukin-6: from basic biology to selective blockade of pro-inflammatory activities. Semin Immunol **26:**2-12.
35. **Zegeye MM, Lindkvist M, Falker K, Kumawat AK, Paramel G, Grenegard M, Sirsjo A, Ljungberg LU.** 2018. Activation of the JAK/STAT3 and PI3K/AKT pathways are crucial for IL-6 trans-signaling-mediated pro-inflammatory response in human vascular endothelial cells. Cell Commun Signal **16:**55.
36. **Zhou F, Xue M, Qin D, Zhu X, Wang C, Zhu J, Hao T, Cheng L, Chen X, Bai Z, Feng N, Gao SJ, Lu C.** 2013. HIV-1 Tat promotes Kaposi's sarcoma-associated herpesvirus (KSHV) vIL-6-induced angiogenesis and tumorigenesis by regulating PI3K/PTEN/AKT/GSK-3β signaling pathway. PLoS One **8:**e53145.
37. **Zhu X, Guo Y, Yao S, Yan Q, Xue M, Hao T, Zhou F, Zhu J, Qin D, Lu C.** 2014. Synergy between Kaposi's sarcoma-associated herpesvirus (KSHV) vIL-6 and HIV-1 Nef protein in promotion of angiogenesis and oncogenesis: role of the AKT signaling pathway. Oncogene **33:**1986-1996.
38. **Aoki Y, Yarchoan R, Wyvill K, Okamoto S, Little RF, Tosato G.** 2001. Detection of viral interleukin-6 in Kaposi sarcoma-associated herpesvirus-linked disorders. Blood **97:**2173-2176.
39. **Brousset P, Cesarman E, Meggetto F, Lamant L, Delsol G.** 2001. Colocalization of the viral interleukin-6 with latent nuclear antigen-1 of human herpesvirus-8 in endothelial spindle cells of Kaposi's sarcoma and lymphoid cells of multicentric Castleman's disease. Hum Pathol **32:**95-100.
40. **Giffin L, Damania B.** 2014. KSHV: pathways to tumorigenesis and persistent infection. Adv Virus Res **88:**111-159.
41. **Punjabi AS, Carroll PA, Chen L, Lagunoff M.** 2007. Persistent activation of STAT3 by latent Kaposi's sarcoma-associated herpesvirus infection of endothelial cells. J Virol **81:**2449-2458.
42. **Li W, Yan Q, Ding X, Shen C, Hu M, Zhu Y, Qin D, Lu H, Krueger BJ, Renne R, Gao SJ, Lu C.** 2016. The SH3BGR/STAT3 Pathway Regulates Cell Migration and Angiogenesis Induced by a Gammaherpesvirus MicroRNA. PLoS Pathog **12:**e1005605.
43. **Chen M, Sun F, Han L, Qu Z.** 2016. Kaposi's sarcoma herpesvirus (KSHV) microRNA K12-1 functions as an oncogene by activating NF-kappaB/IL-6/STAT3 signaling. Oncotarget **7:**33363-33373.
44. **Mongiat M, Andreuzzi E, Tarticchio G, Paulitti A.** 2016. Extracellular Matrix, a Hard Player in Angiogenesis. Int J Mol Sci **17**.
45. **Neve A, Cantatore FP, Maruotti N, Corrado A, Ribatti D.** 2014. Extracellular matrix modulates angiogenesis in physiological and pathological conditions. Biomed Res Int **2014:**756078.
46. **Wang L, Wakisaka N, Tomlinson CC, DeWire SM, Krall S, Pagano JS, Damania B.** 2004. The Kaposi's sarcoma-associated herpesvirus (KSHV/HHV-8) K1 protein induces expression of angiogenic and invasion factors. Cancer Res **64:**2774-2781.

47. **Principe M, Borgoni S, Cascione M, Chattaragada MS, Ferri-Borgogno S, Capello M, Bulfamante S, Chapelle J, Di Modugno F, Defilippi P, Nistico P, Cappello P, Riganti C, Leporatti S, Novelli F.** 2017. Alpha-enolase (ENO1) controls alpha v/beta 3 integrin expression and regulates pancreatic cancer adhesion, invasion, and metastasis. J Hematol Oncol **10:**16.
48. **Aoki Y, Narazaki M, Kishimoto T, Tosato G.** 2001. Receptor engagement by viral interleukin-6 encoded by Kaposi sarcoma-associated herpesvirus. Blood **98:**3042-3049.
49. **Davis ZH, Verschueren E, Jang GM, Kleffman K, Johnson JR, Park J, Von Dollen J, Maher MC, Johnson T, Newton W, Jager S, Shales M, Horner J, Hernandez RD, Krogan NJ, Glaunsinger BA.** 2015. Global mapping of herpesvirus-host protein complexes reveals a transcription strategy for late genes. Mol Cell **57:**349-360.

FIGURE LEGENDS

FIG 1 HUVECs stably expressing vIL-6 have increased ITGB3 mRNA and protein levels. (A) Relative *ITGB3* mRNA expression in stable HUVECs normalized to the expression levels of EV cells. (B) Integrin β3 protein expression in the total cell lysate of stable HUVECs. (C) Top: Relative luciferase expression from a luciferase reporter under the control of an ITGB3-promoter transfected into HEK293T cells. Bottom: Immunoblots for vIL-6 and actin of transfected HEK293T cells. (D) Surface expression of αVβ3 integrin in stable HUVECs was measured using flow cytometry. The gray histogram represents EV HUVECs, and the white histogram represents vIL-6 HUVECs.

FIG 2 vIL-6 induces ITGB3 expression in an intercellular manner. (A and B) hTERT-HUVECs were treated with conditioned medium from EV- or vIL-6-expressing HUVECs for 24 hours, followed by the comparison of ITGB3 mRNA levels (A) and protein expression (B). (C and D) Similar experiments were conducted using conditioned media from EV- and vIL-6-expressing BJABs. (E) Conditioned media were collected from EV- and vIL-6-HUVECs in the presence of non-specific mouse IgG or mouse anti-vIL-6 IgG. This conditioned medium was then placed on hTERT-HUVECs. After 24 hours, lysates were collected and immunoblots performed for actin and integrin β3. CM = condition media; NS = non-specific

FIG 3 STAT3 is necessary for vIL-6-induced ITGB3. (A) EV- and vIL-6-HUVECs were treated with the STAT3 inhibitor cryptotanshinone (0 or 20 μM) for 48 hours. Lysates were then collected and immunoblots performed for the indicated proteins. (B) EV- and

611 vIL-6-HUVECs were transfected with siRNAs for 48 hours, and lysates were probed for
612 the same proteins as in panel A. (C) hTERT-HUVECs were transfected with siRNAs
613 against a non-targeting control or STAT3. Twenty-four hours post-transfection, cells
614 were treated with conditioned medium from EV- or vIL-6-HUVECs and incubated for an
615 additional 24 hours before lysates were collected and used for immunoblots. NTC =
616 non-targeting control; CM = condition media; H = HUVECs
617
618 **FIG 4** Human IL-6 is not a strong inducer of ITGB3 as is vIL-6. (A) Immunoblot of total
619 cell lysates from HUVECs expressing EV, vIL-6, or hIL-6, that were grown for 48 hours
620 in the presence of recombinant hIL-6 at the indicated concentrations. (B) Immunoblot of
621 hTERT-HUVECs treated with conditioned medium from EV-, vIL-6-, and hIL-6-
622 expressing HUVECs and BJABs. (C) Similar to (A), but EV- and vIL-6-HUVECs were
623 grown for 24 hours in the presence of rhIL-6 (250 ng/ml), soluble IL-6Rα, (250ng/ml) or
624 both. rhIL-6 = recombinant hIL-6; CM = condition media; sIL-6R = soluble IL-6Rα.
625
626 **FIG 5** ITGB3 aids in vIL-6 HUVEC adhesion to ECMs. (A) EV- and vIL-6-expressing
627 HUVECs were transfected for 48 hours with non-targeting control or ITGB3 siRNAs, and
628 cell lysates were collected for immunoblots to confirm knockdown efficiency. (B) Cells
629 treated as in panel A were stained with calcein AM and plated for 30 minutes on wells
630 pre-coated with fibronectin. Unattached cells were removed by gentle washes, and
631 fluorescence was measured to quantify the relative amounts of cells adhered to the
632 ECM component. (C) Similar to (B), but with vitronectin-coated wells. Panels B and C

represent the average of three experiments, each with seven technical replicates. NTC = non-targeting control. ***= Kruskal-Wallis test $p<0.001$

FIG 6 ITGB3 contributes to vIL-6-induced tubule formation of endothelial cells. (A) Representative images from four experiments in duplicates done with EV- and vIL-6-expressing HUVECs treated with siRNAs against non-targeting or *ITGB3*. The center of the images was zoomed in for a better resolution of the tubules. (B) The average number of branching points per well (4-5 frames/well) in duplicates was calculated and represented in the scatter plot graph. **= Kruskal-Wallis test $p<0.01$

FIG 7 Model of vIL-6 induction of ITGB3. Expression of vIL-6 augments JAK/STAT3 activation increasing the levels of ITGB3 which results in higher surface expression of the heterodimer αVβ3 integrin. This process promotes vIL-6-induced endothelial cell adhesion to the ECM components fibronectin and vitronectin and promotes tubule formation.

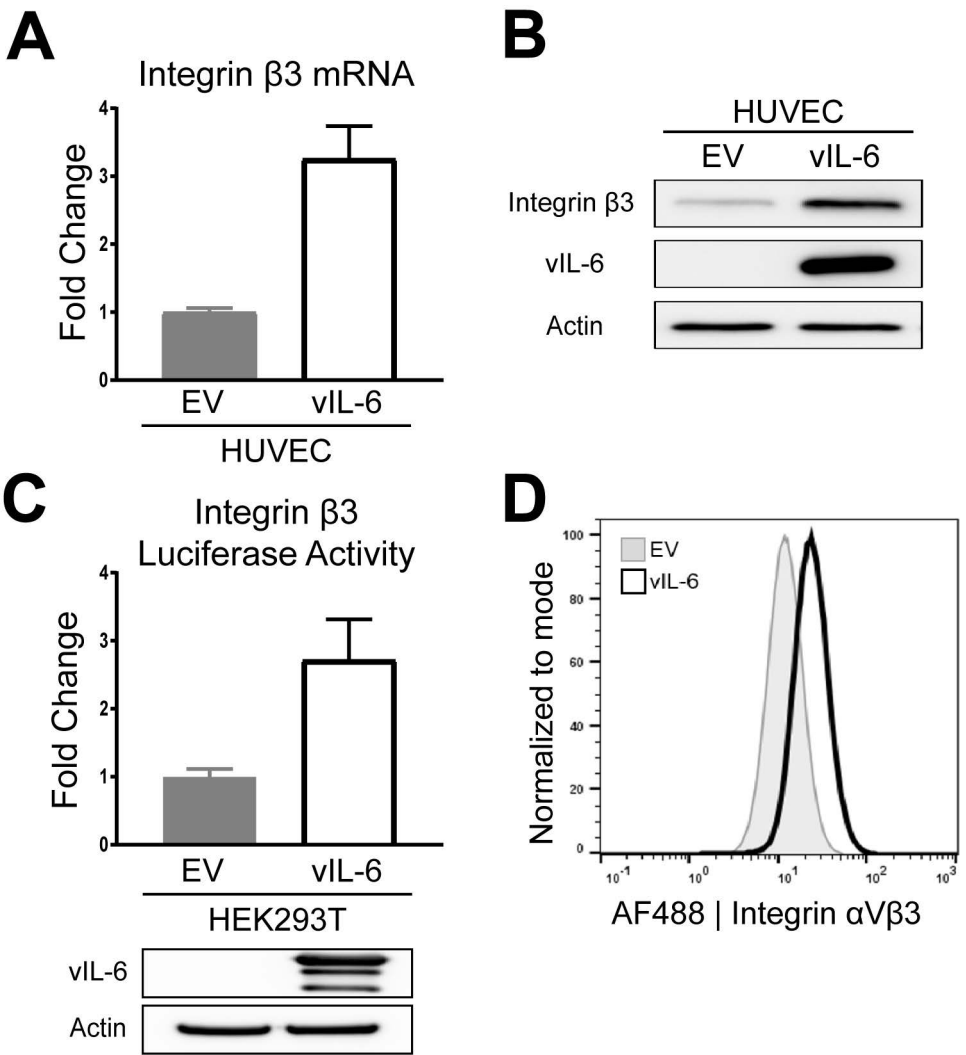
A
Integrin β3 mRNA
Fold Change
4
3
2
1
0
EV
vIL-6
HUVEC
B
HUVEC
EV
vIL-6
Integrin β3
vIL-6
Actin
C
Integrin β3
Luciferase Activity
Fold Change
4
3
2
1
0
EV
vIL-6
HEK293T
vIL-6
Actin
D
Normalized to mode
100
80
60
40
20
0
EV
vIL-6
10^{-1}
10^{0}
10^{1}
10^{2}
10^{3}
AF488 | Integrin αVβ3

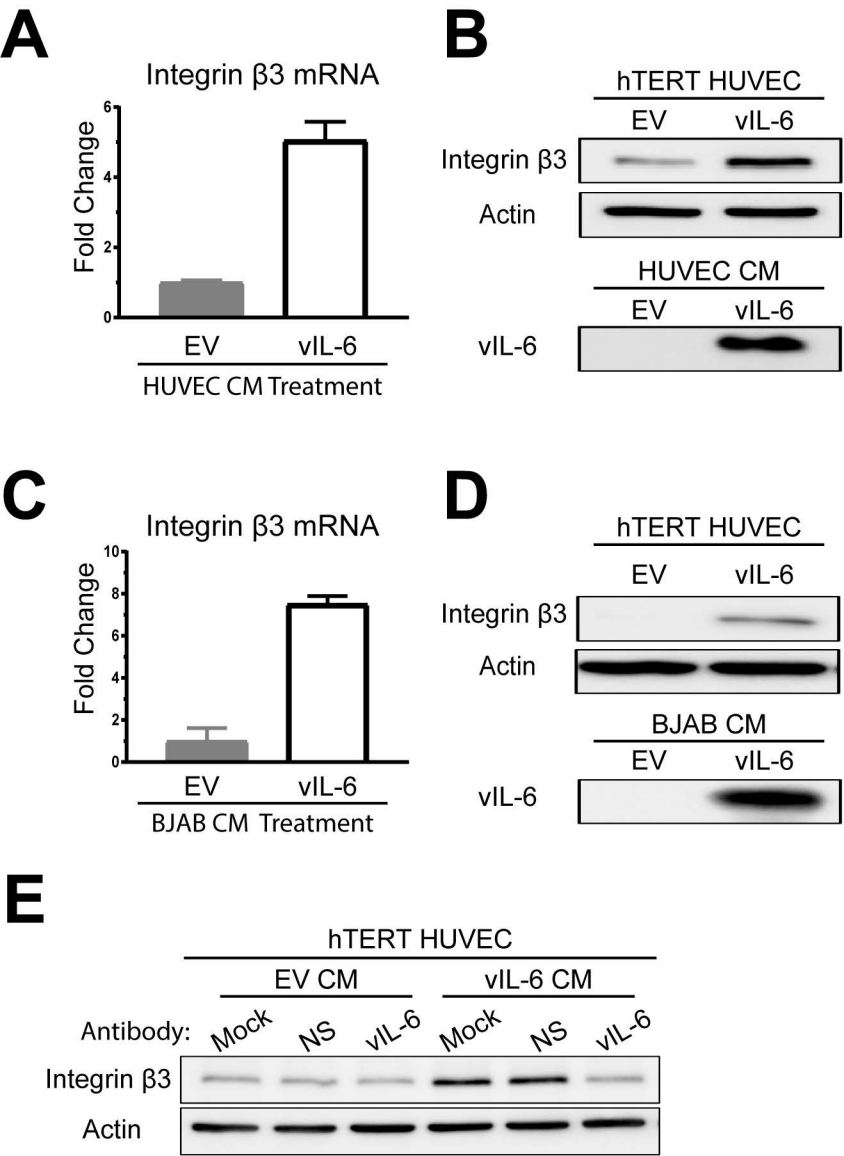
A
Integrin β3 mRNA
Fold Change
6
4
2
0
EV
vIL-6
HUVEC CM Treatment
B
hTERT HUVEC
EV
vIL-6
Integrin β3
Actin
HUVEC CM
EV
vIL-6
vIL-6
C
Integrin β3 mRNA
Fold Change
10
8
6
4
2
0
EV
vIL-6
BJAB CM Treatment
D
hTERT HUVEC
EV
vIL-6
Integrin β3
Actin
BJAB CM
EV
vIL-6
vIL-6
E
hTERT HUVEC
EV CM
vIL-6 CM
Antibody:
Mock
NS
vIL-6
Mock
NS
vIL-6
Integrin β3
Actin

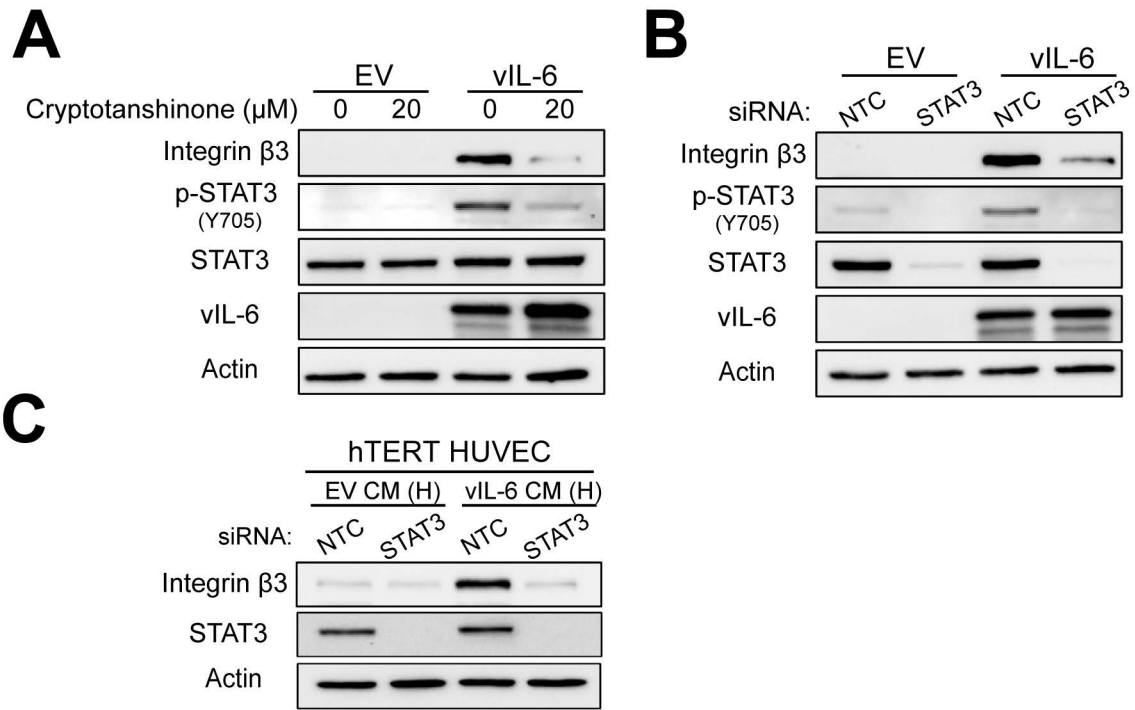
A
EV
vIL-6
Cryptotanshinone (μM)
0
20
0
20
Integrin β3
p-STAT3
(Y705)
STAT3
vIL-6
Actin
B
EV
vIL-6
siRNA:
NTC
STAT3
NTC
STAT3
Integrin β3
p-STAT3
(Y705)
STAT3
vIL-6
Actin
C
hTERT HUVEC
EV CM (H)
vIL-6 CM (H)
siRNA:
NTC
STAT3
NTC
STAT3
Integrin β3
STAT3
Actin

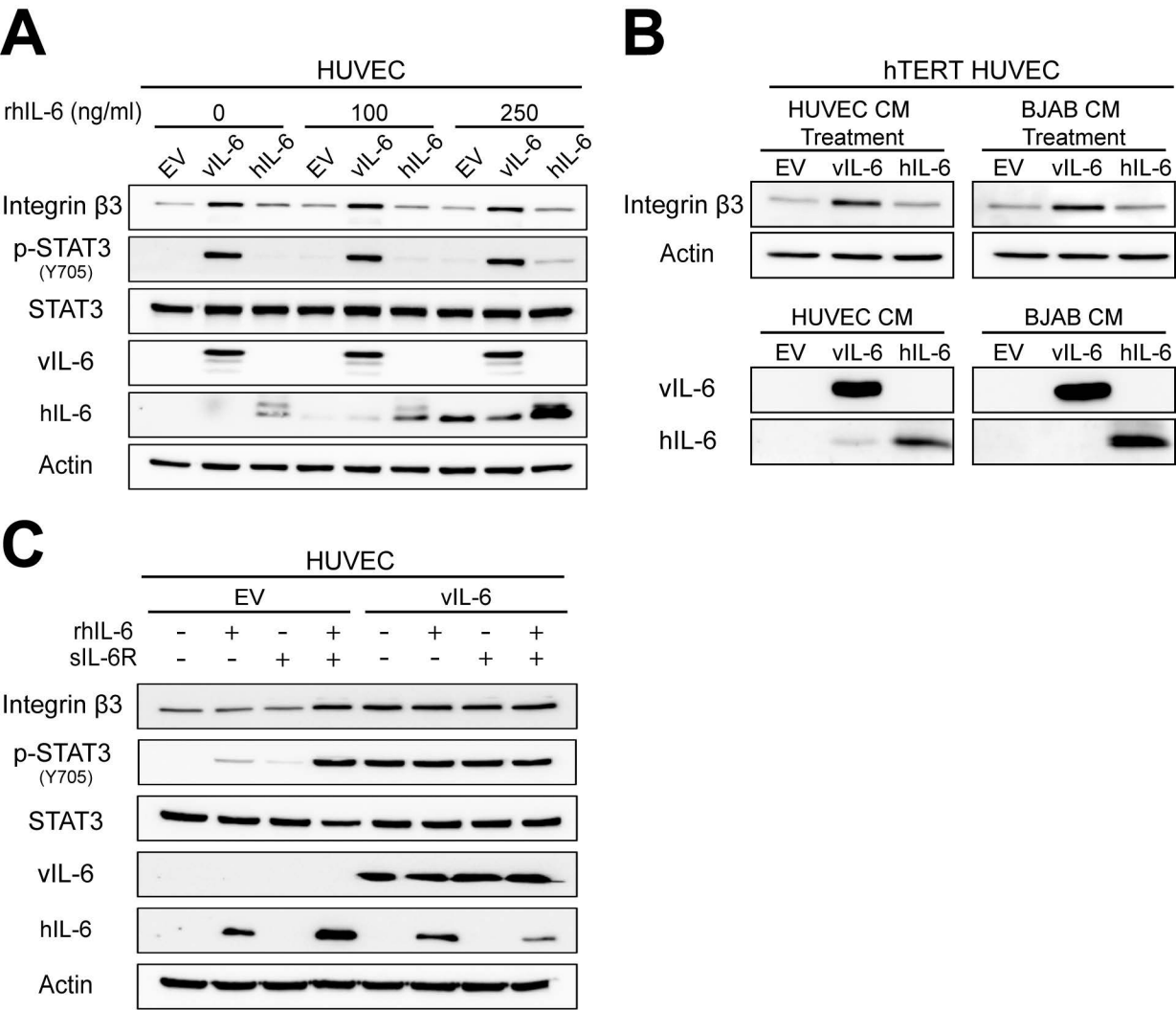
A
HUVEC
rhIL-6 (ng/ml)
0
100
250
EV
vIL-6
hIL-6
Integrin β3
p-STAT3
(Y705)
STAT3
vIL-6
hIL-6
Actin
B
hTERT HUVEC
HUVEC CM
Treatment
BJAB CM
Treatment
Integrin β3
Actin
HUVEC CM
BJAB CM
vIL-6
hIL-6
C
HUVEC
EV
vIL-6
rhIL-6
sIL-6R
Integrin β3
p-STAT3
(Y705)
STAT3
vIL-6
hIL-6
Actin

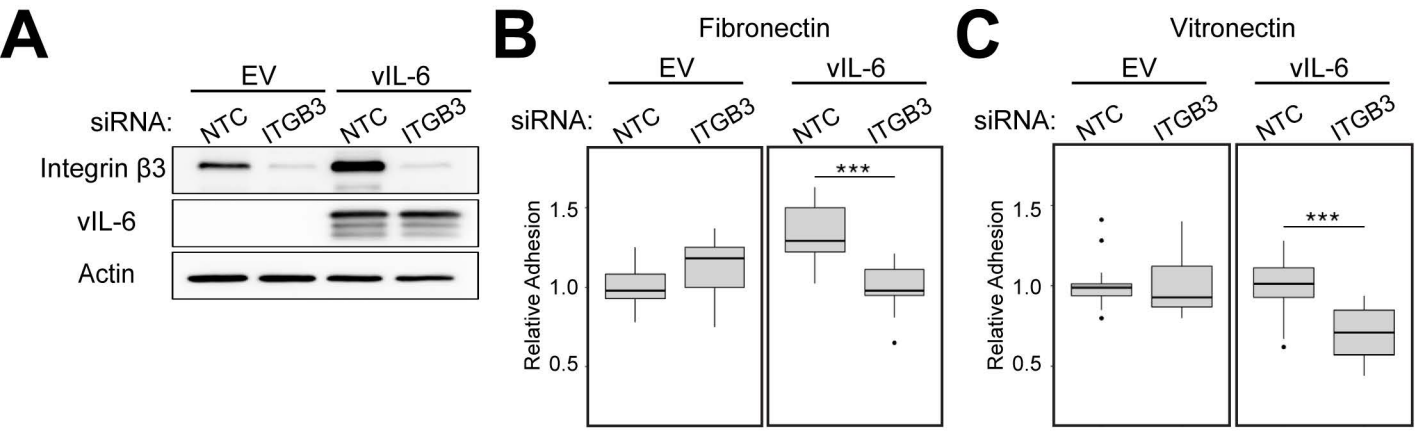
A
EV
vIL-6
siRNA:
NTC
ITGB3
NTC
ITGB3
Integrin β3
vIL-6
Actin
B
Fibronectin
EV
vIL-6
siRNA:
NTC
ITGB3
NTC
ITGB3
Relative Adhesion
1.5
1.0
0.5
***
C
Vitronectin
EV
vIL-6
siRNA:
NTC
ITGB3
NTC
ITGB3
Relative Adhesion
1.5
1.0
0.5
***

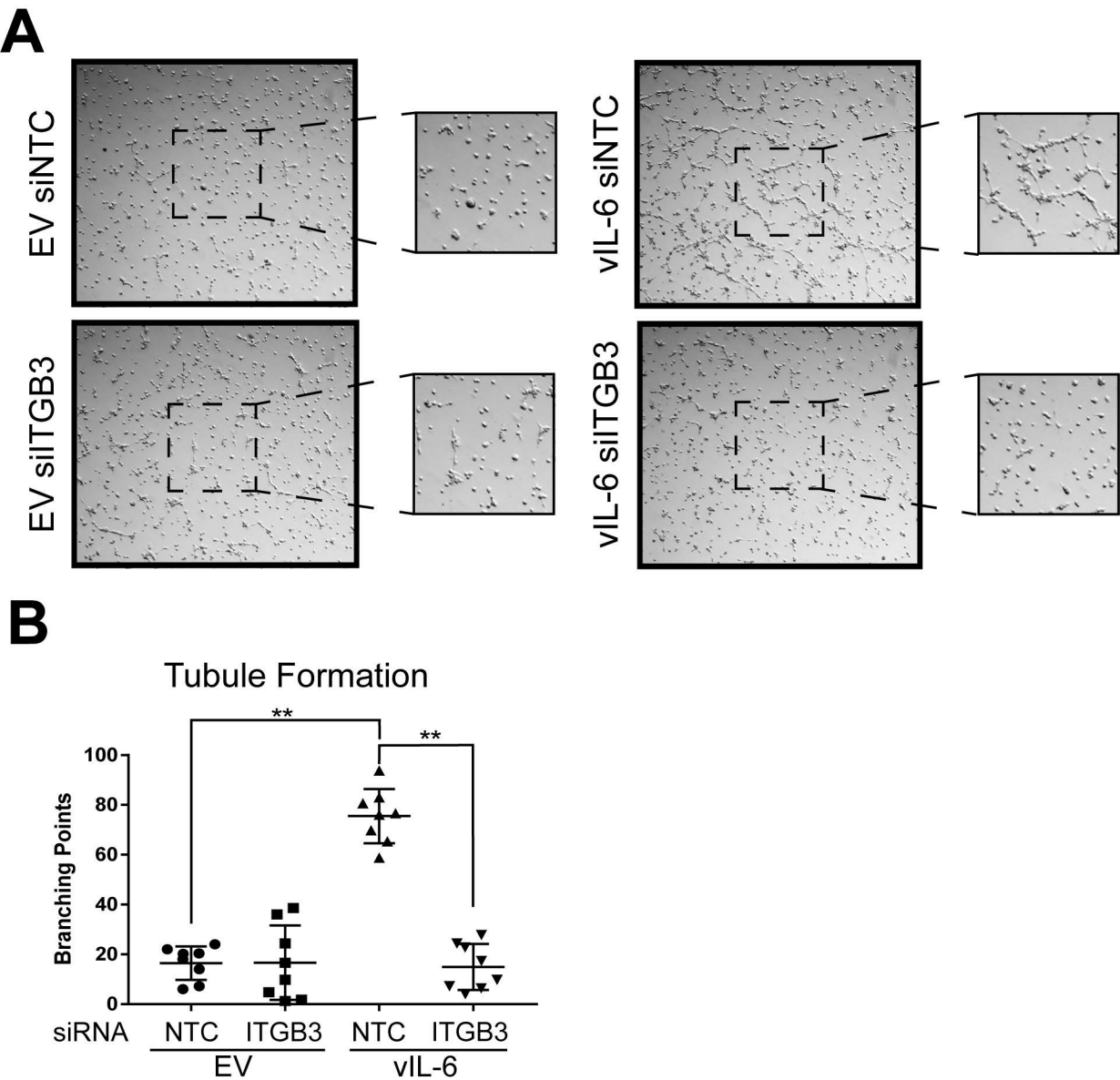
A
EV siNTC
EV siITGB3
vIL-6 siNTC
vIL-6 siITGB3
B
Tubule Formation
**
**
Branching Points
100
80
60
40
20
0
siRNA
NTC
ITGB3
NTC
ITGB3
EV
vIL-6

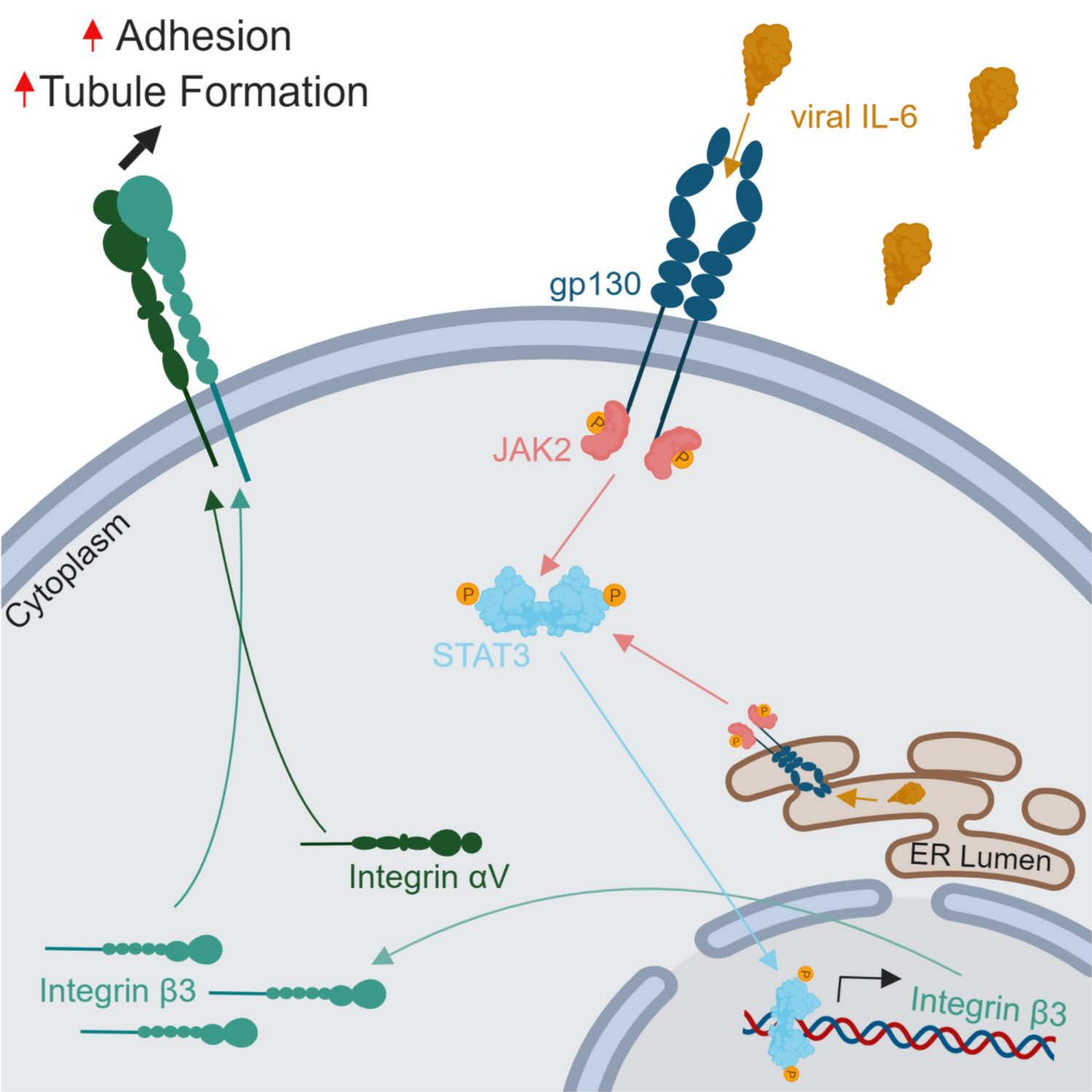
Adhesion
Tubule Formation
viral IL-6
gp130
JAK2
P
Cytoplasm
STAT3
ER Lumen
Integrin αV
Integrin β3
Integrin β3